Production Cross Sections for Lee-Wick Massive Electromagnetic Bosons and for Spin-Zero and Spin-One W Bosons at High Energies*

Ralph Linsker
Department of Physics, Columbia University, New York, New York 10027
and Institute for Space Studies, Goddard Space Flight Center,
National Aeronautics and Space Administration, New York, New York 10025
(Received 26 October 1971)

The total cross section is calculated for the resonant process $l^{\pm}+Z\to l^{\pm}+Z'+B^0\to l^{\pm}+Z'$ + (hadrons or leptons), where $l=\mu$ or e, and B^0 is the hypothetical massive spin-1 boson of electromagnetic interactions, proposed by Lee and Wick. Several (Z,Z') cases have been studied, corresponding to elastic scattering off protons and neutrons (with and without an exclusion principle), coherent scattering off spin-0 nuclei, and inelastic scattering off protons (in which case Z' denotes a nucleon resonance or hadronic system in the continuum). Detailed structure-function data are used to improve the accuracy of the inelastic scattering calculation. At a beam energy of 200–300 GeV, the cross section exceeds 10^{-36} cm^2, provided the B^0 mass is not much greater than 10 GeV. Details of the calculation are given with results for beam energies between 50 and 10 000 GeV and B^0 masses between 5 and 40 GeV. The cross section is also computed for the resonant process $\bar{\nu}_l(\nu_l)+Z\to l^{\pm}+Z'+W_0^{\mp}\to l^{\pm}+Z'$ + (hadrons or leptons) and for the extensively studied semiweak process $\bar{\nu}_l(\nu_l)+Z\to l^{\pm}+Z'$ $+W_1^{\mp}$, where $W_{0,1}^{\pm}$ are the scalar and vector weak intermediate bosons. The cross section for $W_0^{\pm}$ production with $l=\mu$ is found to be at least an order of magnitude smaller than that for $W_1^{\pm}$, in nearly all regions of interest. The $W_0^{\pm}$ production cross section for inelastic scattering off protons is comparable to that for elastic scattering in the regions of interest; whereas in the B^0 and $W_1^{\pm}$ cases, the main contribution to the total cross section for production off protons is elastic.

I. INTRODUCTION

In this paper, production cross sections for three types of hypothetical particles are calculated to lowest order. The processes studied are ($l=\mu$ or e)

$$l^{\pm}+Z\to l^{\pm}+Z'+B^0\searrow \text{hadrons or leptons}, \quad (1.1)$$

where B^0 is the indefinite-metric state associated with the Lee-Wick "heavy-photon pole"[1,2];

$$\bar{\nu}_l(\nu_l)+Z\to l^{\pm}+Z'+W_0^{\mp}\searrow \text{hadrons or leptons}, \quad (1.2)$$

where $W_0^{\pm}$ is the spin-0 weak intermediate boson proposed by Lee[3]; and

$$\bar{\nu}_l(\nu_l)+Z\to l^{\pm}+Z'+W_1^{\mp}, \quad (1.3)$$

where $W_1^{\pm}$ is the usual spin-1 weak intermediate boson. In these reactions Z and Z' denote the initial and final states of the target nucleon or nucleus. The cases treated include elastic scattering off a proton or neutron (either free or embedded within a Fermi sea), coherent scattering off a nucleus, and inelastic scattering off a proton, in which case Z' denotes a nucleon resonance or a hadronic system in the continuum.

It is convenient to treat reactions (1.1)–(1.3) in parallel because they are physically and computationally similar. In each case a lepton scatters off a nucleon or nucleus, via one-photon exchange, producing a heavy boson. The cross sections can be computed accurately to lowest order, since they depend upon well-understood features of the electromagnetic and weak interactions. The strong interaction enters only through the hadronic vertex, which is described empirically for each (Z,Z') combination by appropriate form factors or structure functions; information concerning these vertex functions can be obtained from existing electron scattering experiments.

Because each of the production processes involves a final state consisting of three particles (prior to the decay of the unstable boson), the kinematics are similar for reactions (1.1)–(1.3). The hadronic part of the matrix element depends only on Z and Z', and not on the type of massive boson produced. Consequently, the analytic and numerical methods used to calculate the cross section are similar for the three processes.

In Sec. II, the kinematics, matrix element, and computational method are described for the case of B^0 production [process (1.1)]. In Sec. III, the hadronic vertex is discussed in detail for each (Z,Z') combination considered. In Sec. IV, the calculated cross sections for process (1.1) are presented. In Sec. V, the production of scalar and

vector W bosons via processes (1.2) and (1.3) is discussed, and their respective cross sections compared. Appendix A contains the calculation of the integration limits for B^0 and $W^{\pm}_{0,1}$ production. Appendix B gives results of the trace calculations for the B^0 process.

II. B^0 CALCULATION

As a means of eliminating divergence difficulties in the electrodynamics of hadrons, Lee and Wick[1,2] have proposed that in the electromagnetic interaction Lagrangian the photon field might be described not by the usual amplitude A_μ, but by a complex amplitude $A_\mu + iB_\mu$, where iB_μ is anti-Hermitian. The corresponding B^0 particle is a massive spin-1 boson of indefinite metric. If it exists, it should be observable as a resonance in the production of leptons or hadrons by a lepton scattering off a nucleon or nucleus [process (1.1)]. Possible contributions from diagrams in which the B^0 is emitted by Z or Z', rather than by the lepton, are neglected; the neglect of such diagrams is consistent with gauge invariance.[4] Also, effects due to the possible existence of the massive indefinite-metric fermion field introduced by Lee and Wick[2] have not been considered.

The current lower bound on m_B, obtained from the muon $(g-2)$ measurement and from lepton pair production in proton-uranium scattering, is[5] about 5 GeV. Also, since the observed structure functions W_1 and νW_2 (which depend upon the details of both the nucleon vertex and the photon propagator) are consistent with scaling, one may infer $m_B \gtrsim 9$ GeV,[5] provided one assumes that the vertex part (taken alone) obeys scaling due to the strong interaction.

The cross section for process (1.1) has been given in a previous paper[6] for the cases of elastic scattering of the lepton off a free proton, and coherent scattering off a spin-0 nucleus. In the present paper, the method of calculation is described in detail and the range of validity of the calculations is extended by incorporating inelasticity and exclusion-principle effects, neutron contributions, and an improved treatment of coherent scattering, as described in Sec. III.

A. Lowest-Order Matrix Element

The interaction Lagrangian of the B^0 with the lepton is anti-Hermitian,[1,2] and is given by[7]

$$\mathcal{L}_{\rm int}(B^0) = e\psi^{\dagger}\gamma_4\gamma_\lambda\psi B_\lambda, \tag{2.1}$$

where ψ and B denote the lepton and B^0 fields. The two lowest-order Feynman diagrams in which the B^0 is emitted by the lepton are given in Fig. 1. We denote the mass of the lepton by m_l; of the B^0, by m_B; of Z, by M; and of Z', by M'. The four-momentum of the incoming lepton is called k; of the outgoing lepton, k'; of the B^0, k_B; of Z, p; and of Z', p'. All of these momenta are on the mass shell; thus $k^2 = k'^2 = -m_l^2$, $k_B^2 = -m_B^2$, $p^2 = -M^2$, and $p'^2 = -M'^2$. The last of these constraints will appear explicitly in the expression for the cross section [Eq. (2.8)].

Defining the four-momentum transfer $q = p' - p$, the matrix element $\mathfrak{M}$ for the lowest-order process is then

$$\mathfrak{M} = K_\sigma V_\sigma, \tag{2.2}$$

where

$$K_\sigma = -ie^2\bar{u}'[(\beta')^{-1}(-q_\nu\gamma_\lambda\gamma_\nu\gamma_\sigma + 2k_\sigma\gamma_\lambda) + \beta^{-1}(q_\nu\gamma_\sigma\gamma_\nu\gamma_\lambda + 2k'_\sigma\gamma_\lambda)]uB_\lambda, \tag{2.3}$$

$$\beta' = (k-q)^2 + m_l^2, \quad \beta = (k'+q)^2 + m_l^2, \tag{2.4}$$

and V_σ denotes the interaction with the nucleon or nucleus. Here u and u' are the respective spinors of the incoming and outgoing leptons, normalized so that $\bar{u}u = \bar{u}'u' = 2m_l$. The amplitude of the B^0, denoted by B_λ, satisfies

$$\sum B_\lambda B_\kappa = \delta_{\lambda\kappa} + k_{B\lambda}k_{B\kappa}/m_B^2, \tag{2.5}$$

where the sum extends over the three polarization states of the B^0.

The factorization (2.2) of $\mathfrak{M}$ into leptonic and hadronic parts occurs because the diagrams of Fig. 1 involve one-photon exchange. The total cross sections of interest will be seen [Eq. (2.8)] to depend on V_σ only through the combination[7]

$$\sum_h{}' V_\sigma V_\tau^{\star}\delta(p'^2 + M'^2) = (2Me^2/q^4)W_{\sigma\tau}, \tag{2.6}$$

where $\sum'_h$ denotes the average over the spin (if any) of the target particle Z, and the summation over allowed final states and spins of Z'. [For any four-vector $a = (\vec{a}, ia_0)$, $a^{\star}$ is defined as $(\vec{a}^*, ia_0^*)$, where $*$ denotes ordinary complex conju-

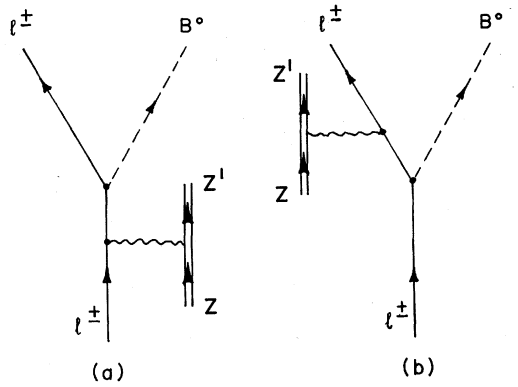

FIG. 1. Feynman diagrams for B^0 production.

gation.] In Sec. III, $W_{\sigma\tau}$ is given for each (Z, Z') combination treated. $W_{\sigma\tau}$ depends only upon p and q, $W_{\sigma\tau}=W_{\tau\sigma}$, and (by gauge invariance) $q_\sigma W_{\sigma\tau}=0$; therefore $W_{\sigma\tau}$ can be written as[8]

$$W_{\sigma\tau}=W_1\left(\delta_{\sigma\tau}-\frac{q_\sigma q_\tau}{q^2}\right)+\frac{W_2}{M^2}\left(p_\sigma-\frac{p\cdot q}{q^2}\,q_\sigma\right)\left(p_\tau-\frac{p\cdot q}{q^2}\,q_\tau\right), \tag{2.7}$$

where the structure functions $W_{1,2}$ depend upon q^2 and $p\cdot q$ only.

It should be noted that any modification of the photon propagator due to the possible existence of B^0 enters also into the empirical determination of the hadronic structure functions, and therefore need not be considered separately.

B. Phase-Space Integration

The total cross section, assuming the incoming beam or target to be unpolarized and summing over all allowed final states Z' and over all spins of outgoing particles, is given by

$$\sigma=(512\pi^5 M|\vec{k}|_{\rm lab})^{-1}\int\sum_l{}'\sum_h{}'[|\mathfrak{M}|^2\delta(p'^2+M'^2)]X(q^2)\delta^{(4)}(k-k'-k_B-q)\,d^4p'\left(\frac{d^3k'}{k_0'}\right)\left(\frac{d^3k_B}{k_{B0}}\right). \tag{2.8}$$

Here $\sum_l'$ denotes the average over initial lepton spin and summation over final lepton and B^0 spins. $X(q^2)$ denotes a possible exclusion-principle suppression factor, discussed in Sec. III.

If the integrations of Eq. (2.8) were to be carried out in the laboratory frame, special procedures would be required to handle the extreme peaking of the integrand in several of the variables. This peaking arises from two causes. First, at the beam energies of interest (several hundred GeV and higher) there is a strong relativistic peaking in the forward direction. In addition, the photon propagator, the lepton propagator, and the hadronic electromagnetic form factors all favor the virtual photon and the virtual lepton to be near their respective mass shells. As a result, the integrand tends to "blow up" over very small kinematic domains. [Of the two lepton propagator denominators β and β' in Eq. (2.3), β' is rather slowly varying since $|\beta'|\geq m_B{}^2$, which is taken to be large. However, the propagator denominator β has a minimum value of $O(q^2)$ if one neglects terms in m_l.]

We therefore follow the procedure of evaluating two of the integrals in the frame $\vec{k}'=-\vec{k}_B$. By the proper choice of variables it then becomes possible to perform two of the integrations analytically, and the remaining two integrations (or three, if the mass M' of the final hadron system assumes a continuous range of values) to any desired accuracy using a rapid and straightforward numerical scheme.

First d^4p' is calculated in the lab frame. Defining $t=q^2$, $u=k\cdot q$, and $\phi_{p'}$ equal to the azimuthal angle of $\vec{p}'$ (about the polar axis $\vec{k}$), we have

$$d^4p'=d^4q=(4M|\vec{k}|_{\rm lab})^{-1}\,dt\,du\,dp'^2\,d\phi_{p'}. \tag{2.9}$$

Next, the Lorentz-invariant quantity

$$I=\frac{d^3k'\,d^3k_B\,\delta^{(4)}(k_0-k_0'-k_{B0}-q_0)}{k_0'\,k_{B0}} \tag{2.10}$$

is evaluated in the frame $\vec{k}'=-\vec{k}_B$. Three of the momentum-conservation δ functions are used to eliminate d^3k_B. Defining ϕ' as the azimuthal angle of $\vec{k}'$ (about the polar axis $\vec{k}$), we obtain

$$I=\tfrac{1}{2}(u^2+m_l{}^2t)^{-1/2}\,d\beta\,d\phi'. \tag{2.11}$$

Defining

$$L_{\sigma\tau}=\frac{1}{e^4}\sum_l{}'K_\sigma K_\tau^*, \tag{2.12}$$

the total cross section is then given by

$$\sigma=\frac{\alpha^3}{32\pi^2 M|\vec{k}|_{\rm lab}{}^2}\times\int\frac{L_{\sigma\tau}W_{\sigma\tau}X(t)\,dt\,du\,dp'^2\,d\phi_{p'}\,d\beta\,d\phi'}{t^2(u^2+m_l{}^2t)^{1/2}}. \tag{2.13}$$

The limits of integration are given in Appendix A.

The $\phi_{p'}$ integration in Eq. (2.13) is trivial. The double integral

$$N_{\sigma\tau}=\iint L_{\sigma\tau}\,d\beta\,d\phi' \tag{2.14}$$

depends only upon k and q, and since $L_{\sigma\tau}=L_{\tau\sigma}$ and $q_\sigma L_{\sigma\tau}=0$, we may write

$$N_{\sigma\tau}=N_A\left(\delta_{\sigma\tau}-\frac{q_\sigma q_\tau}{t}\right)+N_B\left(k_\sigma-\frac{u}{t}\,q_\sigma\right)\left(k_\tau-\frac{u}{t}\,q_\tau\right), \tag{2.15}$$

where N_A and N_B are linear combinations of $N_{\sigma\sigma}$ and $k_\sigma N_{\sigma\tau}k_\tau$.

The expressions for $L_{\sigma\sigma}$ and $k_\sigma L_{\sigma\tau}k_\tau$ are given in Appendix B. They were calculated in invariant form, using Veltman's symbolic manipulation program SCHOONSCHIP[9] to perform some of the tedious algebra. Since $\beta^2 L_{\sigma\sigma}$ and $\beta^2 k_\sigma L_{\sigma\tau}k_\tau$ are independent of ϕ' and are polynomials in β, N_A

and N_B are easily calculated.

The remaining integrations are done numerically using an iterative adaptive scheme for multiple Simpson integration. To reduce the number of iterations required for convergence, the outermost integration is over t, the variable in which the integrand varies most rapidly. In the case of coherent scattering off nuclei, the integration over t is transformed into one over a new variable (described in Sec. III) to assure a more efficient placement of points.

III. HADRONIC VERTEX

Several distinct cases for (Z, Z') are considered. For each case the structure functions W_1 and W_2 are given. The factor $X(q^2)$ [Eqs. (2.8) and (2.13)] is unity except in case B below. The laboratory frame is defined in each case as the frame in which the target is initially at rest ($\vec{p}=0$).

A. Elastic Scattering

For elastic scattering off a free nucleon, the familiar dipole fit[10] is sufficiently accurate for our purposes:

$$F_1(q^2) = G_{Ep}[z+\kappa(1+4M^2/q^2)^{-1}],$$
$$F_2(q^2) = \tfrac{1}{2} G_{Ep}\kappa(1+q^2/4M^2)^{-1}, \tag{3.1}$$

where

$$G_{Ep} = (1+q^2/0.71)^{-2}, \quad q \text{ in GeV},$$
$$z = \begin{cases} 0 & \text{for neutrons} \\ 1 & \text{for protons}, \end{cases} \tag{3.2}$$
$$\kappa = \begin{cases} -1.913 & \text{for neutrons} \\ 1.7928 & \text{for protons}. \end{cases}$$

Then

$$V_\sigma = (ie/q^2)\bar{u}_{p'}[F_1\gamma_\sigma + \tfrac{1}{2} iF_2M^{-1}(\gamma_\sigma\gamma_\beta - \gamma_\beta\gamma_\sigma)q_\beta]u_p, \tag{3.3}$$

where u_p and $u_{p'}$ are the spinors of the initial and final nucleons, with $\bar{u}_p u_p = \bar{u}_{p'} u_{p'} = 2M$. W_1 and W_2, defined by Eqs. (2.6) and (2.7), are given by

$$W_1 = (q^2/2M)(F_1+2F_2)^2\delta(M^2+p'^2),$$
$$W_2 = 2(F_1^2M + F_2^2t/M)\delta(M^2+p'^2). \tag{3.4}$$

The cross sections computed using these structure functions are denoted by σ_p and σ_n, for elastic scattering off free protons and neutrons, respectively.

B. Exclusion Principle

We consider the case of elastic scattering off a nucleon embedded within a Fermi sea. The form factors are identical to those of case A above, but collisions involving small three-momentum transfer $\vec{q}_{\rm lab}$ are suppressed by the exclusion principle. For an ideal Fermi gas the suppression factor is[11,12]

$$X(q^2) = \begin{cases} 1.5(|\vec{q}|/2p_f) - 0.5(|\vec{q}|/2p_f)^3, & |\vec{q}| \le 2p_f \\ 1, & |\vec{q}| > 2p_f. \end{cases} \tag{3.5}$$

We use $p_f = 235$ MeV/c for the numerical calculations[12]; this corresponds to a nucleon density similar to that within a nucleus.

The cross sections corresponding to this case are denoted by σ'_p and σ'_n, for protons and neutrons, respectively.

C. Coherent Scattering

For the case of coherent scattering off a spin-0 nucleus of charge Z, we have

$$V_\sigma = (eZ/q^2)(p+p')_\sigma F(q^2); \tag{3.6}$$

thus

$$W_1 = 0,$$
$$W_2 = 2MZ^2F^2\delta(M^2+p'^2). \tag{3.7}$$

In the Breit frame ($q_0=0$) we assume the Fermi charge distribution used by Lǿvseth and Radomski[12]:

$$\rho_F(r) \propto (1+e^{(r-r_0)/c})^{-1}, \tag{3.8}$$

with $r_0 = (1.18A^{1/3} - 0.48)$ F, and $c = 0.55$ F. ρ_F is normalized such that $\int \rho_F(r)\, d^3r = 1$. The form factor is given by the Fourier transform in the Breit frame,

$$F_F(q^2) = \int \rho_F(r) e^{i\vec{q}\cdot\vec{r}}\, d^3r. \tag{3.9}$$

The contribution of collisions with squared four-momentum transfers $q^2 \gtrsim 0.25$ GeV^2 to the total cross section is very small[12,13] for the B^0 masses and beam energies of interest. For the numerical calculations we therefore impose the arbitrary but convenient cutoff used by Brown and Smith[13]:

$$F(q^2) = F_F(q^2)\theta(0.25 \text{ GeV}^2 - q^2). \tag{3.10}$$

In order to ensure that the integrand $d\sigma/dq^2$ is computed at values of q^2 which are efficiently chosen with respect to the positions of the diffraction maxima and minima, we transform the integral to one over the new variable

$$x = \int_{q^2}^{\infty} F^2(t')\, dt' \tag{3.11}$$

used by Lǿvseth and Radomski.[12] The resulting Jacobian cancels $F^2(q^2)$ in the integrand. A table of corresponding q^2 and x values is generated for each nucleus of interest, and q^2 is obtained by interpolation at each point x of evaluation of the in-

tegrand.

We denote the cross section for coherent scattering with the Fermi form factor (3.10) by $\sigma_{\rm coh}$.

If the cross section is known for coherent scattering off two different nuclei, Løvseth and Radomski[12] suggest using the interpolative formula

$$\sigma_{\rm coh} = c_1/a^2 + c_2 \tag{3.12}$$

to calculate the cross section for a nucleus with an intermediate atomic weight A. Here a is the rms nuclear radius

$$a = (0.58 + 0.82A^{1/3})\ \text{F}, \tag{3.13}$$

and c_1 and c_2 are constants to be fit to the two nuclei for which $\sigma_{\rm coh}$ is given.

For the sake of comparison with the literature,[6,14] we shall also consider some results of computations of coherent scattering using the dipole form factor

$$F_{\rm dip}(q^2) = (1 + \tfrac{1}{12}a^2q^2)^{-2}, \tag{3.14}$$

with

$$a = (\tfrac{3}{5})^{1/2}(1.3A^{1/3})\ \text{F}. \tag{3.15}$$

The corresponding cross section is denoted by $\sigma_{\rm coh,dip}$. We note that $F_{\rm dip}(q^2)$ is generally larger than $|F_{\rm F}(q^2)|$.

Recent electron scattering data reported by Sick and McCarthy[15] strongly favor the choice of the Fermi form factor $F_{\rm F}(q^2)$, in preference to a dipole or exponential fit. Excellent agreement through the first diffraction minimum can be clearly observed in these data.

D. Inelastic Scattering Off Protons

We consider the case of inelastic scattering off a proton, where the final state Z' is a nucleon resonance or a state in the hadronic continuum. In this case the structure functions W_1 and W_2 depend in general upon both q^2 and the mass M' of the outgoing hadron system. In the region $q^2 \gtrsim 1$ GeV^2, $M' \gtrsim 2.6$ GeV, the e-p scattering data are consistent with the empirical scaling law[16]

$$\nu W_2 = \left(1 - \frac{1}{\omega}\right)^3\left[1.274 + 0.5989\left(1 - \frac{1}{\omega}\right) - 1.675\left(1 - \frac{1}{\omega}\right)^2\right], \tag{3.16}$$

where $\nu \equiv q_{0,\rm lab} = (q^2 + M'^2 - M^2)/2M$ and $\omega = 2M\nu/q^2$. The νW_2 data obey a scaling law down to $M' \approx 1.8$ GeV if the variable $\omega' = \omega + M^2/q^2$, introduced by Bloom and Gilman,[17] is used[16]:

$$\nu W_2 = \left(1 - \frac{1}{\omega'}\right)^3\left[0.6453 + 1.902\left(1 - \frac{1}{\omega'}\right) - 2.343\left(1 - \frac{1}{\omega'}\right)^2\right]. \tag{3.17}$$

For either Eq. (3.16) or Eq. (3.17), W_1 is approximately given by[16]

$$W_1 = \frac{W_2}{1+R}\left(1 + \frac{\nu^2}{q^2}\right), \tag{3.18}$$

$$R = 0.18, \tag{3.19}$$

where R is the ratio of longitudinal to transverse virtual photoabsorption cross sections.

Scaling in either ω or ω' cannot be strictly valid near nucleon resonances, since the resonance peaks occur at fixed values of M'. However, the results of Bloom and Gilman[17] suggest that scaling in ω' holds to a good approximation down to threshold ($M' = M + m_\pi$) provided that $q^2 > 1$ GeV^2. We therefore use Eqs. (3.17)–(3.19) in the numerical computations, for $q^2 > 1$ GeV^2 and all M'.

For 0.1 GeV$^2 \leq q^2 \leq 1$ GeV^2 and $M' \leq 4.7$ GeV, we calculate νW_2 by linear interpolation in q^2 and M', using new νW_2 tables obtained from the SLAC-MIT collaboration.[18] A portion of these values is presented in Fig. 2. Since νW_2 becomes essentially independent of M' at the largest M' values given in the SLAC-MIT tables, it is reasonable for our purposes to make the approximate extrapolation

$$\nu W_2(q^2, M') = \nu W_2(q^2, 4.7\ \text{GeV}), \quad \text{for} \tag{3.20}$$

$$0.1 \leq q^2 \leq 1\ \text{GeV}^2, \quad M' > 4.7\ \text{GeV}.$$

W_1 is calculated using Eq. (3.18) with $R = 0.15$.

For $q^2 < 0.1$ GeV^2 we proceed as follows. At $q^2 = 0$, $\nu W_2 = 0$ and W_1 is related to the photoabsorption cross section $\sigma_{\gamma p}$ by

$$W_1 = (\nu/4\pi^2\alpha)\sigma_{\gamma p}. \tag{3.21}$$

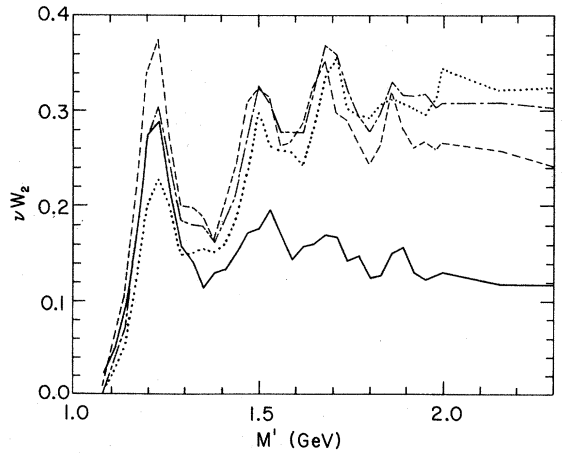

FIG. 2. Structure function νW_2 from SLAC-MIT inelastic e-p scattering data (Ref. 18), for four-momentum transfer squared $q^2 = 0.1$ (—), 0.4 (---), 0.7 (-·-), and 1.0 GeV^2 (···).

For $M' \leq 4.7$ GeV, we therefore calculate both W_1 and νW_2 by interpolating linearly in q^2 and M', using the $q^2 = 0$ photoabsorption data[19] and $q^2 = 0.1$ GeV^2 SLAC-MIT data.[18] (The ratio R is not constrained in this case; it varies from 0.15 at $q^2 = 0.1$ GeV^2 to zero at $q^2 = 0$.) We note that at large M' (up to 4.7 GeV), $\sigma_{\gamma p}$ is essentially independent of M'. It is consistent to make the approximate extrapolation

$$\nu W_2(q^2, M') = \nu W_2(q^2, 4.7 \text{ GeV}),$$
$$\frac{1}{\nu} W_1(q^2, M') = \frac{1}{\nu} W_1(q^2, 4.7 \text{ GeV}), \tag{3.22}$$

for

$$q^2 < 0.1 \text{ GeV}^2, \quad M' > 4.7 \text{ GeV}.$$

The cross section for inelastic scattering off protons is denoted by σ_{inel}.

E. Unspecified Final Hadron State

If no restrictions are placed upon the composition of the final hadronic state, then the total cross section for scattering off a free proton is given by

$$\sigma_{p,\text{tot}} = \sigma_p + \sigma_{\text{inel}}. \tag{3.23}$$

The total cross section for scattering off a compound nucleus is more difficult to estimate. The total contribution due to coherent and quasielastic scattering off a nucleus containing Z protons and N neutrons is given approximately by[20,21]

$$\sigma_{\text{nuc}} = \sigma_{\text{coh}} + Z\sigma'_p + N\sigma'_n. \tag{3.24}$$

The additional contribution due to inelastic scattering off the constituent protons can be estimated as $Z\sigma_{\text{inel}}$. This ignores corrections arising from the exclusion principle, which are difficult to determine because of the indefinite composition of the final hadron state in this case.

Recent results for inelastic electron scattering off deuterium[22] suggest that the structure function νW_2 is likely to be somewhat smaller for neutrons than for protons.

TABLE I. Calculated cross sections in units of 10^{-38} cm^2, for B^0 production [process (1.1)] with $l = \mu$. In Tables I–V, σ_p and σ_n refer to elastic scattering off a free proton and a free neutron; σ'_p and σ'_n refer to elastic scattering off a proton or neutron which is within an appropriate Fermi sea; σ_{inel} refers to inelastic scattering off a free proton; and σ_{coh} refers to coherent scattering off a spin-0 nucleus.

m_B (GeV)	$E_{\mu,\text{in}}$ (GeV)	σ_p	σ'_p	σ_n	σ'_n	σ_{inel}	$\frac{1}{6}\sigma_{\text{coh}}$ (C)	$\frac{1}{26}\sigma_{\text{coh}}$ (Fe)	$\frac{1}{82}\sigma_{\text{coh}}$ (Pb)
5	50	325	323	104	104	73.1	0.384	0.490	0.251
	100	1890	1700	383	354	621	208	57.3	42.2
	150	3610	2950	553	491	1330	1320	1040	264
	200	5210	3960	661	575	2030	3300	4150	1710
	300	7980	5460	790	672	3290	8660	16 200	13 600
	400	10 300	6510	864	728	4370	14 700	32 600	37 400
	700	15 500	8450	974	810	6820	31 800	87 700	145 000
	1000	19 200	9540	1020	848	8590	46 600	140 000	265 000
7	50	3.89	3.89	1.69	1.69	0.510	...	...	...
	100	228	226	72.7	72.1	65.3	0.331	0.413	0.203
	150	669	632	164	156	235	22.0	6.67	3.99
	200	1170	1050	234	215	455	144	43.0	29.4
	300	2170	1770	328	290	925	849	716	189
	400	3100	2340	386	335	1380	2060	2720	1220
	700	5360	3490	478	405	2530	7000	14 800	15 600
	1000	7100	4210	522	438	3420	12 300	30 500	43 000
10	100	2.70	2.70	1.19	1.19	0.498	...	...	...
	150	42.9	42.9	16.3	16.3	12.4	0.0174	0.0139	0.006 55
	200	129	128	42.0	41.7	44.4	0.161	0.205	0.101
	300	370	350	91.8	87.5	152	11.2	3.52	2.01
	400	642	574	130	120	286	75.0	21.8	15.1
	700	1430	1120	197	173	706	747	810	266
	1000	2120	1520	232	199	1090	1910	3160	2110
13	150	0.590	0.590	0.267	0.267	0.101	...	...	...
	200	8.30	8.30	3.47	3.47	2.32	3.93×10^{-4}	1.86×10^{-4}	1.48×10^{-4}
	300	59.0	58.9	20.6	20.6	21.5	0.0354	0.0378	0.0240
	400	141	137	41.1	40.2	58.7	0.806	0.657	0.296
	700	443	393	87.2	80.0	218	59.8	19.5	12.1
	1000	747	611	115	102	391	279	228	59.3

IV. B^0 RESULTS

A. Beam Energies $\leq$ 1000 GeV

In Table I we present calculated total cross sections for process (1.1) with $l=\mu$ at B^0 masses of 5, 7, 10, and 13 GeV, and at incoming muon energies $E_{\mu,\text{in}} \equiv k_{0,\text{lab}}$ up to 1000 GeV. The designations σ_p, σ_p', σ_n, σ_n', σ_{inel}, and σ_{coh} refer to the cross sections for the (Z, Z') cases discussed in Sec. III. The results for coherent scattering are given for three types of target nuclei: ${}_6C^{12}$, ${}_{26}Fe^{56}$, and ${}_{82}Pb^{208}$.

In Fig. 3(a), σ_p, $\frac{1}{6}\sigma_{\text{coh}}(C)$, and $\frac{1}{82}\sigma_{\text{coh}}(Pb)$ are plotted versus $E_{\mu,\text{in}}$ for $m_B=7$ and 13 GeV. In Fig. 3(b), σ_p, σ_p', σ_n, and σ_n' are given for $m_B=5$ and 13 GeV. In Fig. 3(c), σ_p and σ_{inel} are given for $m_B=7$ and 10 GeV.

We list several key results of the calculations.

1. σ_p is greater than σ_n for all cases studied, typically by a factor of 5 and 10 [see Fig. 3(b)].

2. At a beam energy of 300 GeV, σ_p is several times as large as $\sigma_{\text{coh}}(Z)/Z$ for $m_B \geq 7$ GeV, but is smaller than $\sigma_{\text{coh}}(Z)/Z$ for $m_B=5$ GeV. At 1000 GeV, the maximum beam energy considered, σ_p is less than $\sigma_{\text{coh}}(Z)/Z$ for $m_B \lesssim 10$ GeV [Fig. 3(a)].

3. At $E_{\mu,\text{in}}=1000$ GeV, $\sigma_{\text{coh}}(Z)/Z$ increases with Z for $m_B \lesssim 7$ GeV, but decreases with increasing Z for $m_B \gtrsim 13$ GeV [Fig. 3(a)]. This is not surprising since, closer to threshold, the main contribution to the cross section comes from larger values of q^2, and the coherent form factor generally drops with Z more rapidly at larger q^2.

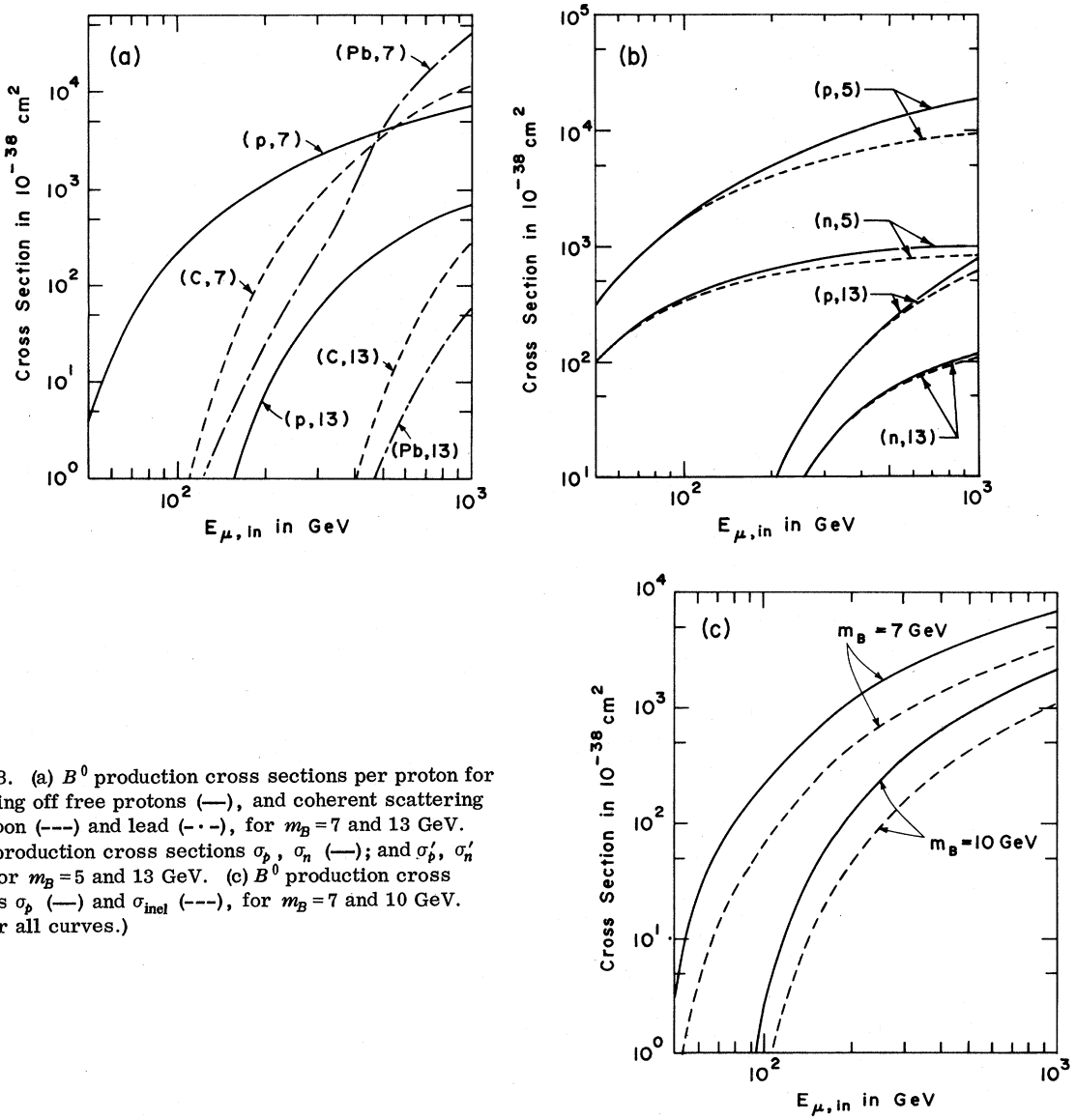

FIG. 3. (a) B^0 production cross sections per proton for scattering off free protons (—), and coherent scattering off carbon (---) and lead (-·-), for $m_B=7$ and 13 GeV. (b) B^0 production cross sections σ_p, σ_n (—); and σ_p', σ_n' (---); for $m_B=5$ and 13 GeV. (c) B^0 production cross sections σ_p (—) and σ_{inel} (---), for $m_B=7$ and 10 GeV. ($l=\mu$ for all curves.)

4. The cross section $\sigma_{\text{coh,dip}}$ (calculated according to a dipole form factor) is as much as several times as great as σ_{coh} (obtained using a Fermi form factor), particularly near threshold. Even at $E_{\mu,\text{in}}=1000$ GeV, $\sigma_{\text{coh,dip}}/\sigma_{\text{coh}}$ for ${}_{26}\text{Fe}^{56}$ varies from 1.08 at $m_B=5$ GeV to 2.75 at $m_B=13$ GeV. This is not surprising since $F_{\text{dip}}(q^2)$ is generally much larger[23] than $|F_F(q^2)|$ except for very small values of q^2 – which are kinematically inaccessible for $E_{\mu,\text{in}}$ near threshold.

5. The extent to which the exclusion principle suppresses the cross section for scattering off protons [i.e., the quantity $(\sigma_p-\sigma_p')/\sigma_p$] increases with beam energy up to about 20% at $m_B=13$ GeV, and up to 50% at $m_B=5$ GeV (for $E_{\mu,\text{in}}=1000$ GeV). [See Fig. 3(b).] This is also a result of the fact that smaller q^2 values are attainable further from threshold.

6. The exclusion-principle suppression effect is qualitatively similar for neutrons and protons. However, the extent of the suppression varies over a narrower range for neutrons – from 11% at $m_B=13$ GeV to 17% at $m_B=5$ GeV (for $E_{\mu,\text{in}}=1000$ GeV [Fig. 3(b)].

7. The ratio $\sigma_{\text{inel}}/\sigma_p$ increases approximately from 20% to 50% over the range of $E_{\mu,\text{in}}$ considered. It is not strongly dependent upon m_B. [See Fig. 3(c).]

8. The detailed treatment which we have given for the $q^2\leq 1$ GeV^2 region is necessary for an accurate calculation of σ_{inel}. If instead of using the photoabsorption and SLAC-MIT data, one assumes scaling in ω' [Eq. (3.17)] for *all* q^2 and M', one obtains cross sections for inelastic scattering which are typically about 30% greater than those given in Table I. Because smaller q^2 values become more important further from threshold, the error resulting from the assumption of universal scaling is greater far from threshold; e.g., about 33% at $m_B=5$ GeV, compared with 26% at $m_B=13$ GeV and $E_{\mu,\text{in}}=700$ GeV, and with 7% at $m_B=13$ GeV and $E_{\mu,\text{in}}=200$ GeV.

If one uses Eq. (3.17) for all q^2 and M', the further effect of changing R from 0.18 to zero is to increase the inelastic cross sections by approximately 3–12%.

B. Results at Higher Energies

Recent colliding-beam developments raise the possibility of attaining much greater c.m. energies in e-p scattering experiments than can be achieved at the National Accelerator Laboratory. For example, for electron and proton beam energies of 15 and 200 GeV, respectively, the c.m. energy corresponds to that which would be achieved by a 6-TeV electron beam incident on a fixed proton.

We present below the cross section for process (1.1) with $l=e$, for beam energies $E_{e,\text{in}}$ measured in the proton rest frame, and for[24] $m_B=37.29$ GeV. We find for

$$E_{e,\text{in}}=1\text{ TeV},\ 5\text{ TeV},\ \text{and}\ 10\text{ TeV},$$
$$\sigma_p=0.008\,84,\ 61.6,\ \text{and}\ 169,\qquad(4.1)$$
and
$$\sigma_{\text{inel}}=0.001\,83,\ 38.1,\ \text{and}\ 109,$$

respectively, where σ_p and σ_{inel} are in units of 10^{-38} cm^2.

V. SCALAR AND VECTOR $W^{\pm}$ PRODUCTION

Cross sections for production of the scalar W boson ($W_0^{\pm}$) via process (1.2) have recently been reported.[25] The present paper extends these results in one or more of the following ways: (a) A more detailed treatment of the hadronic vertex is given; (b) two integrations are done analytically, enabling one to obtain cross sections accurate to $\approx$1% after several seconds of calculation (on an IBM 360/95); (c) the case in which the scalar and vector $W^{\pm}$ masses are unequal is treated correctly; and (d) all lepton mass terms are retained.

The cross section for vector W-boson ($W_1^{\pm}$) production [process (1.3)] has been extensively discussed in the literature,[11,13,14,21,26] on the assumption that the $W_0^{\pm}$ does not exist. Since all modifications to the $W_1^{\pm}$ cross section arising from the existence of $W_0^{\pm}$ vanish in the limit of zero lepton mass,[3] it is not surprising to find (see Reiff[25]) that for nonzero lepton mass, the $W_1^{\pm}$ cross section is quite insensitive to the existence of the $W_0^{\pm}$. We therefore neglect effects due to $W_0^{\pm}$ in calculating the $W_1^{\pm}$ process. This calculation (a) provides a check of the computational procedures used; (b) is useful for comparing the $W_0^{\pm}$ and $W_1^{\pm}$ results; and (c) gives new results for the case of inelastic scattering off protons.

A. Lowest-Order Matrix Element

The Feynman diagrams for process (1.2) or (1.3) are given in Fig. 4 to lowest order, according to the renormalizable weak-intermediate-boson theory proposed by Lee.[3] The matrix element is[7]

$$\mathfrak{M}=K_\sigma' V_\sigma,\qquad(5.1)$$

where

$$K'_\sigma = ig n_\tau \bar{u}_l \left(e\gamma_\sigma \frac{(k'+q)\cdot\gamma + im_l}{(k'+q)^2 + m_l^2}\gamma_\tau - \gamma_\lambda [V'_\sigma(k_W, k_W+q)]_{\tau\rho} D_{\lambda\rho}(k_W+q) \right)(1+\gamma_5)u_{\nu_l}. \tag{5.2}$$

k, k', and k_W are the respective four-momenta of the incident neutrino, the outgoing lepton, and the W boson (all of which are on their mass shells); m_l, m_0, and m_1 are the masses of the lepton, the $W_0^\pm$, and the $W_1^\pm$; V_σ characterizes the interaction at the hadronic vertex (see Sec. III); u_l and u_{ν_l} are the lepton and neutrino spinors, with $\bar{u}_l u_l = 2m_l$ and $u^\dagger_{\nu_l} u_{\nu_l} = 2k_0$; $q \equiv p' - p$, where p and p' are the respective four-momenta of the target particle Z and its final state Z'; and

$$n_\tau = \begin{cases} i(k_W)_\tau / m_1 & \text{for } W_0^\pm \text{ production} \\ \varphi_\tau & \text{for } W_1^\pm \text{ production}, \end{cases} \tag{5.3}$$

where φ_τ is the polarization vector of the $W_1^\pm$, normalized in the same way as B_λ [see Eq. (2.5)].

The W-boson propagator, which is represented by the zig-zag line in Fig. 4, is given by [Eq. (12) of Ref. 3]

$$D_{\mu\nu}(l) = \frac{\delta_{\mu\nu}}{l^2 + m_1^2} + \frac{l_\mu l_\nu}{m_1^2}\left(\frac{1}{l^2 + m_1^2} - \frac{1}{l^2 + m_0^2} \right), \tag{5.4}$$

and the vertex for $W_\nu \to W_\mu + \gamma$ is [Eq. (18) of Ref. 3]

$$[V'_\lambda(l', l)]_{\mu\nu} = e\{\delta_{\mu\nu}(l+l')_\lambda + [(m_1/m_0)^2 + \kappa](\delta_{\lambda\mu} l_\nu + \delta_{\lambda\nu} l'_\mu) - (1+\kappa)(\delta_{\lambda\mu} l'_\nu + \delta_{\lambda\nu} l_\mu)\}, \tag{5.5}$$

where l and l' are the respective four-momenta of the initial W_ν and the final W_μ, and κ is related to the magnetic moment $\overline{M}$ of $W_1^\pm$ by [Eq. (19) of Ref. 3]

$$\overline{M} = (e/2m_1)(1+\kappa)(\text{spin}). \tag{5.6}$$

The matrix element for process (1.2) in the limit of zero lepton mass m_l has been given by Lee[3]; it is

$$\mathfrak{M} = \frac{eg}{m_1(m_1^2 - 2k\cdot k')} \bar{u}_l [(1-\kappa)(q\cdot W V\cdot\gamma - q\cdot\gamma W\cdot V) + q^2 V\cdot\gamma](1+\gamma_5)u_{\nu_l}, \tag{5.7}$$

where we have made use of gauge invariance ($q\cdot V = 0$)

In the limit $m_0 \to \infty$, the matrix element for process (1.3) reduces to that given by Lee, Markstein, and Yang.[14]

B. Phase-Space Integration

The method of calculation is analogous to that used for the B^0 process. With the substitution $k_B \to k_W$, the total cross section (for an unpolarized target) is given by Eq. (2.8), and the variables p'^2, t, u, ϕ'_p, β, ϕ' are defined as in Sec. II. The limits of integration for these variables are changed slightly from the B^0 case (since the incoming and outgoing leptons now have unequal masses); these changes are given in Appendix A. (The results of the SCHOONSCHIP trace calculations are too lengthy to reproduce here.) Although the analytic integration over β can still be done in a straightforward manner, it is complicated in the $W_0^\pm$ case by the fact that three denominators in K'_σ [Eq. (5.2)] are functions of β [i.e., β, $(2u-\beta)$, and $(2u-\beta-m_0^2+m_1^2)$], while only one denominator depends upon β in the B^0 calculation, and two depend upon β in the $W_1^\pm$ case.

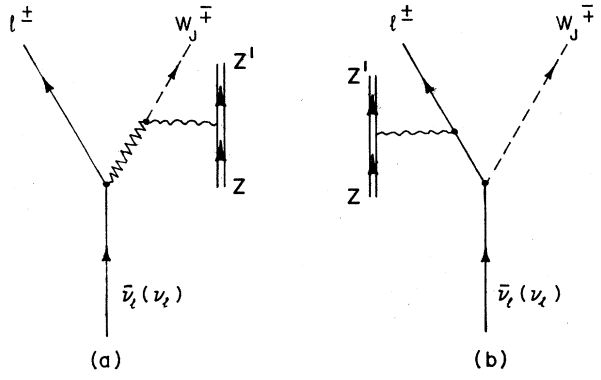

FIG. 4. Feynman diagrams for $W_J^\pm$ production ($J=0$ or 1).

C. Results

In this section we present calculated cross sections for $W_0^\pm$ production [process (1.2)] and $W_1^\pm$ production [process (1.3)], with $l = \mu$, for the (Z, Z') cases discussed in Sec. III. (For coherent scattering, the nuclei used are $_{10}Ne^{20}$, $_{26}Fe^{56}$, and

$_{82}Pb^{208}$.) Table II gives the cross section for $W_0^\pm$ production with $m_1 = 5$ GeV and $m_0 = 2.5$ GeV, and for $W_1^\pm$ production with $m_1 = 5$ GeV and $m_0 = \infty$. (The $W_1^\pm$ cross sections, as mentioned above, are not expected to depend strongly upon m_0, since the lepton mass m_l is small.) Table III gives $W_0^\pm$ production cross sections for $m_0 = m_1 = 5$ GeV; and Table IV is similar to Table II except that $m_1 = 10$ GeV, $m_0 = 5$ GeV for $W_0^\pm$ production, and $m_1 = 10$ GeV, $m_0 = \infty$ for $W_1^\pm$ production. In Table V we give $W_0^\pm$ cross sections for the case of zero lepton mass, at $m_0 = m_1 = 5$ GeV and $E_\nu = 200$ GeV. In Tables II-V the $W_0^\pm$ cross sections have been given for the three cases $\kappa = \pm 1, 0$ (which suffice since the cross section is quadratic in κ). Results for $W_1^\pm$ production are given for the case $\kappa = 0$. (The variation of the cross section with κ is much less for $W_1^\pm$ than for $W_0^\pm$.)

In Fig. 5(a), σ_p, $\frac{1}{10}\sigma_{coh}$(Ne), and $\frac{1}{82}\sigma_{coh}$(Pb) are plotted versus $E_\nu \equiv k_{0,lab}$ for $W_0^\pm$ production with $m_1 = 5$ GeV and $m_0 = 2.5$ GeV, and for $W_1^\pm$ production with $m_1 = 5$ GeV. In Fig. 5(b), σ_p, σ_p', σ_n, and σ_n' are given for $W_0^\pm$ production with $m_1 = 10$ GeV and $m_0 = 5$ GeV, and for $W_1^\pm$ production with $m_1 = 10$ GeV. In Fig. 5(c), σ_p and σ_{inel} are given for $W_0^\pm$ production with $m_1 = 5$ GeV for the two cases $m_0 = 2.5$ and 5 GeV, and for $W_1^\pm$ production with $m_1 = 5$ GeV. (All plotted results are for $\kappa = 0$.)

We list some noteworthy aspects of the results.

1. The cross section for $W_1^\pm$ production is typically at least an order of magnitude greater than that for $W_0^\pm$ production (except near the $W_1^\pm$ threshold when $m_0 < m_1$). It is possible to understand this in a rough way in certain kinematic regions. The

TABLE II. Cross sections (units of 10^{-38} cm^2) for $W_0^\pm$ production [process (1.2)] with $m_1 = 5$ GeV, $m_0 = 2.5$ GeV; and for $W_1^\pm$ production [process (1.3)] with $m_1 = 5$ GeV. ($l = \mu$ in Tables II–IV.)

E_ν (GeV)	Spin of W boson produced	κ	σ_p	σ_p'	σ_n	σ_n'	σ_{inel}	$\frac{1}{10}\sigma_{coh}$(Ne)	$\frac{1}{26}\sigma_{coh}$(Fe)	$\frac{1}{82}\sigma_{coh}$(Pb)
50	1	0	3.09	3.07	1.00	0.998	0.721	0.005 89	0.004 46	0.002 29
	0	−1	0.547	0.515	0.155	0.150	0.305	0.0458	0.0317	0.0119
		0	0.152	0.141	0.0410	0.0395	0.0957	0.0229	0.0195	0.007 66
		+1	0.0357	0.0291	0.005 08	0.004 63	0.0391	0.0206	0.0200	0.007 67
100	1	0	18.2	16.4	3.80	3.52	6.27	1.56	0.524	0.386
	0	−1	2.23	1.98	0.518	0.491	1.53	0.636	0.672	0.438
		0	0.586	0.514	0.133	0.126	0.464	0.214	0.256	0.213
		+1	0.0781	0.0570	0.009 09	0.008 32	0.204	0.111	0.171	0.190
150	1	0	35.1	29.0	5.65	5.05	13.7	13.2	9.36	2.43
	0	−1	4.40	3.76	0.910	0.854	3.29	2.07	2.56	2.22
		0	1.14	0.962	0.231	0.217	0.988	0.617	0.821	0.842
		+1	0.111	0.0768	0.0120	0.0111	0.468	0.213	0.374	0.559
200	1	0	51.2	39.5	6.92	6.08	21.4	37.2	38.2	15.7
	0	−1	6.80	5.64	1.30	1.21	5.38	4.27	5.75	5.85
		0	1.74	1.43	0.328	0.305	1.60	1.20	1.71	1.95
		+1	0.138	0.0921	0.0143	0.0133	0.801	0.307	0.578	0.991
300	1	0	79.8	55.8	8.61	7.44	35.7	108	148	125
	0	−1	11.9	9.42	2.02	1.86	10.0	10.4	15.5	18.8
		0	3.01	2.38	0.508	0.469	2.94	2.80	4.28	5.58
		+1	0.180	0.115	0.0180	0.0168	1.60	0.472	0.946	1.87
400	1	0	104	68.0	9.73	8.34	48.6	193	304	347
	0	−1	17.0	13.1	2.68	2.46	15.0	18.3	28.7	38.6
		0	4.29	3.29	0.672	0.617	4.34	4.79	7.68	10.8
		+1	0.213	0.132	0.0208	0.0196	2.54	0.608	1.26	2.67
700	1	0	161	92.3	11.7	9.97	80.1	454	834	1360
	0	−1	31.8	23.0	4.34	3.94	30.5	47.0	80.7	127
		0	8.01	5.78	1.09	0.988	8.59	12.2	20.8	33.8
		+1	0.282	0.167	0.0268	0.0255	5.79	0.915	1.99	4.65

Feynman diagram of Fig. 4(a) contributes propagator denominators $D_i=(k-k')^2+m_i^2$ $(i=0,1)$; that of Fig. 4(b) contributes $D'=(k-k_W)^2+m_i^2$. Neglecting terms of $O(m_i^2)$, we have $D_i \geq m_i^2$, whereas D' can be of $O(q^2)$. However [except for terms of $O(m_i^2)$], the denominator D' is canceled by numerator terms in the expression for the $W_0^\pm$ cross section [see Eq. (5.7)] but not in the $W_1^\pm$ case. Therefore, when D' achieves sufficiently small values, and when consequently Fig. 4(b) is dominant over Fig. 4(a) for the $W_1^\pm$ case (in the usual gauge), it is to be expected that $W_1^\pm$ production will dominate over $W_0^\pm$ production.

2. The $W_0^\pm$ cross section is suppressed for $\kappa=1$. This is plausible in view of Eq. (5.7), which shows that, except for lepton mass terms and terms of $O(q^2)$, the matrix element is proportional to $1-\kappa$. Also, the suppression is more severe for σ_p than for σ_{inel}.

3. The approximation $m_i=0$ is unreliable for $W_0^\pm$ calculations, particularly for $\kappa=1$ and for coherent scattering (with any κ). This may be related to the fact that all terms $\propto(D')^{-1}$ vanish when lepton mass is ignored.

4. The ratio $\sigma_{\text{inel}}/\sigma_p$ is considerably greater for $W_0^\pm$ production than for $W_1^\pm$ (or B^0) production, and in fact we have $\sigma_{\text{inel}}>\sigma_p$ in some $W_0^\pm$ cases, particularly when $\kappa=1$. This may occur because inelastic cross sections fall off with q^2 more slowly than elastic cross sections, and because the matrix element for $\kappa=1$ is proportional to q^2 (except for lepton mass terms).

Since inelastic scattering is of such importance for $W_0^\pm$ production, the value of using detailed structure function data at low q^2 (rather than using a universal scaling law) is apparent.

5. Several of the features described above have been reported independently by Reiff.[25] Specifically, he notes the dominance of $W_1^\pm$ over $W_0^\pm$ production, the suppression of the $W_0^\pm$ cross section for $\kappa=1$, and the fact that $m_i=0$ is generally not a valid approximation for the $W_0^\pm$ computations. However, Reiff states (incorrectly) that for the masses and energies discussed, the $W_0^\pm$ cross section sometimes increases with increasing m_0 (for m_1 fixed). [See his result (iv).] This statement is based upon his numerical results which omit a factor of $(m_1/m_0)^2$. There is no evidence, either in Reiff's values after correction, or in the present results, to suggest that the $W_0^\pm$ cross section does not decrease with increasing m_0.

Note added in proof. The total cross sections reported by Turner and Barish (Ref. 25) for $W_0^\pm$ production by neutrinos agree with the present calculations, provided the same form factors are used. Turner and Barish use the dipole form fac-

TABLE III. Cross sections (units of 10^{-38} cm^2) for $W_0^\pm$ production with $m_0=m_1=5$ GeV.

E_ν (GeV)	κ	σ_p	σ_p'	σ_n	σ_n'	σ_{inel}	$\frac{1}{10}\sigma_{\text{coh}}$(Ne)	$\frac{1}{26}\sigma_{\text{coh}}$(Fe)	$\frac{1}{82}\sigma_{\text{coh}}$(Pb)
50	−1	0.0531	0.0530	0.0215	0.0215	0.0222	2.06×10^{-5}	1.08×10^{-5}	6.31×10^{-6}
	0	0.0136	0.0136	0.005 53	0.005 53	0.006 29	5.47×10^{-6}	2.98×10^{-6}	1.72×10^{-6}
	+1	0.001 39	0.001 39	0.000 36	0.000 36	0.001 18	1.95×10^{-6}	1.48×10^{-6}	7.24×10^{-7}
100	−1	0.626	0.612	0.206	0.202	0.392	0.005 53	0.002 64	0.001 68
	0	0.158	0.154	0.0520	0.0511	0.110	0.001 45	6.84×10^{-4}	4.38×10^{-4}
	+1	0.009 91	0.009 46	0.001 99	0.001 93	0.0287	0.000 39	1.41×10^{-4}	9.91×10^{-5}
150	−1	1.70	1.61	0.484	0.468	1.24	0.0877	0.0444	0.0187
	0	0.428	0.405	0.122	0.118	0.345	0.0224	0.0115	0.004 75
	+1	0.0204	0.0189	0.003 75	0.003 62	0.108	0.003 16	0.002 20	0.000 59
200	−1	3.09	2.85	0.792	0.755	2.42	0.376	0.253	0.0965
	0	0.776	0.716	0.199	0.190	0.673	0.0949	0.0644	0.0247
	+1	0.0308	0.0278	0.005 39	0.005 21	0.242	0.008 68	0.008 57	0.003 62
300	−1	6.40	5.64	1.41	1.33	5.47	1.84	1.76	0.862
	0	1.60	1.41	0.354	0.334	1.51	0.462	0.444	0.219
	+1	0.0493	0.0432	0.008 22	0.007 96	0.650	0.0246	0.0327	0.0273
400	−1	10.1	8.56	2.00	1.87	9.08	4.55	5.17	3.54
	0	2.52	2.14	0.502	0.468	2.49	1.14	1.30	0.892
	+1	0.0650	0.0559	0.0106	0.0103	1.21	0.0430	0.0653	0.0741
700	−1	21.6	17.1	3.56	3.27	21.3	18.6	26.3	28.1
	0	5.40	4.27	0.891	0.818	5.73	4.64	6.57	7.03
	+1	0.102	0.0846	0.0160	0.0155	3.45	0.0976	0.174	0.281

TABLE IV. Cross sections (units of 10^{-38} cm^2) for $W_0^{\pm}$ production with $m_1 = 10$ GeV, $m_0 = 5$ GeV; and for $W_1^{\pm}$ production with $m_1 = 10$ GeV.

E_ν (GeV)	Spin of W boson produced	κ	σ_p	σ'_p	σ_n	σ'_n	σ_{inel}	$\frac{1}{10}\sigma_{\text{coh}}$ (Ne)	$\frac{1}{26}\sigma_{\text{coh}}$ (Fe)	$\frac{1}{82}\sigma_{\text{coh}}$ (Pb)
50 [a]	0	−1	0.005 73	0.005 73	0.002 34	0.002 34	0.002 28	2.38×10^{-6}	1.44×10^{-6}	7.97×10^{-7}
		0	0.001 79	0.001 79	6.94×10^{-4}	6.93×10^{-4}	7.30×10^{-4}	1.37×10^{-6}	1.04×10^{-6}	5.07×10^{-7}
		+1	0.000 67	0.000 66	2.03×10^{-4}	2.02×10^{-4}	2.14×10^{-4}	1.31×10^{-6}	9.94×10^{-7}	5.12×10^{-7}
100	1	0	0.101	0.101	0.0441	0.0441	0.0189	...	...	...
	0	−1	0.0887	0.0870	0.0306	0.0302	0.0541	6.64×10^{-4}	3.13×10^{-4}	1.97×10^{-4}
		0	0.0242	0.0236	0.008 06	0.007 93	0.0159	3.69×10^{-4}	1.44×10^{-4}	9.83×10^{-5}
		+1	0.004 07	0.003 70	0.000 80	0.000 75	0.003 92	3.38×10^{-4}	1.11×10^{-4}	8.32×10^{-5}
150	1	0	1.60	1.60	0.607	0.607	0.470	9.15×10^{-4}	5.00×10^{-4}	2.36×10^{-4}
	0	−1	0.280	0.270	0.0866	0.0842	0.199	0.009 76	0.005 04	0.002 12
		0	0.0736	0.0702	0.0222	0.0216	0.0577	0.004 07	0.002 49	8.44×10^{-4}
		+1	0.008 04	0.006 77	0.001 27	0.001 15	0.0147	0.002 79	0.001 97	5.16×10^{-4}
200	1	0	4.82	4.79	1.58	1.56	1.70	0.008 59	0.007 41	0.003 55
	0	−1	0.561	0.528	0.159	0.154	0.434	0.0438	0.0291	0.0109
		0	0.145	0.136	0.0406	0.0392	0.125	0.0154	0.0117	0.004 63
		+1	0.0118	0.009 46	0.001 64	0.001 48	0.0337	0.007 74	0.007 90	0.003 33
300	1	0	13.9	13.2	3.50	3.34	5.90	0.237	0.127	0.0731
	0	−1	1.32	1.20	0.333	0.319	1.12	0.238	0.214	0.106
		0	0.337	0.306	0.0842	0.0804	0.324	0.0708	0.0698	0.0411
		+1	0.0187	0.0139	0.002 23	0.002 02	0.0962	0.0221	0.0305	0.0261
400	1	0	24.2	21.8	5.01	4.64	11.2	2.28	0.792	0.549
	0	−1	2.26	2.01	0.525	0.497	2.04	0.642	0.669	0.433
		0	0.574	0.507	0.132	0.125	0.585	0.179	0.199	0.145
		+1	0.0247	0.0175	0.002 71	0.002 46	0.188	0.0388	0.0612	0.0715
700	1	0	55.0	43.6	7.90	6.98	28.6	32.1	29.5	9.68
	0	−1	5.63	4.73	1.11	1.04	5.57	3.13	4.07	3.86
		0	1.42	1.19	0.279	0.261	1.59	0.825	1.10	1.11
		+1	0.0386	0.0252	0.003 79	0.003 48	0.595	0.0884	0.164	0.273

[a] This energy is below threshold for production of 10-GeV vector W bosons.

tor [Eqs. (3.14) and (3.15)] to calculate coherent cross sections; their results are therefore in some cases considerably larger than the σ_{coh} values given in Tables II–V, which are based upon the form factor of Eq. (3.10). (The discussion given in result 4 of Sec. IV applies qualitatively to the $W_0^{\pm}$ case as well.)

TABLE V. Cross sections (units of 10^{-38} cm^2) for $W_0^{\pm}$ production with zero lepton mass, $m_0 = m_1 = 5$ GeV, and $E_\nu = 200$ GeV.

κ	−1	0	+1
σ_p	3.12	0.782	0.0214
σ'_p	2.87	0.719	0.0208
σ_n	0.795	0.200	0.004 25
σ'_n	0.758	0.191	0.004 23
σ_{inel}	2.43	0.676	0.239
$\frac{1}{10}\sigma_{\text{coh}}$ (Ne)	0.391	0.0978	9.13×10^{-4}
$\frac{1}{26}\sigma_{\text{coh}}$ (Fe)	0.271	0.0678	5.80×10^{-4}
$\frac{1}{82}\sigma_{\text{coh}}$ (Pb)	0.0947	0.0237	2.24×10^{-4}

ACKNOWLEDGMENTS

I am indebted to Professor T. D. Lee for suggesting this problem, and for essential advice and encouragement throughout the course of the work. I have profited from discussions with Professor N. H. Christ and with Dr. R. W. Brown, who also supplied me with a copy of the SCHOONSCHIP program; and from correspondence with Dr. H. H. Chen. I also thank Allan Rothenberg for informing me of the SLAC-MIT data, arranging to have them supplied to me in preliminary form, and for useful discussions. I thank Dr. William Cooper, Dr. Jack Smith, and Dr. J. Reiff for discussions and confirmational work on the $W_0^{\pm}$ process.

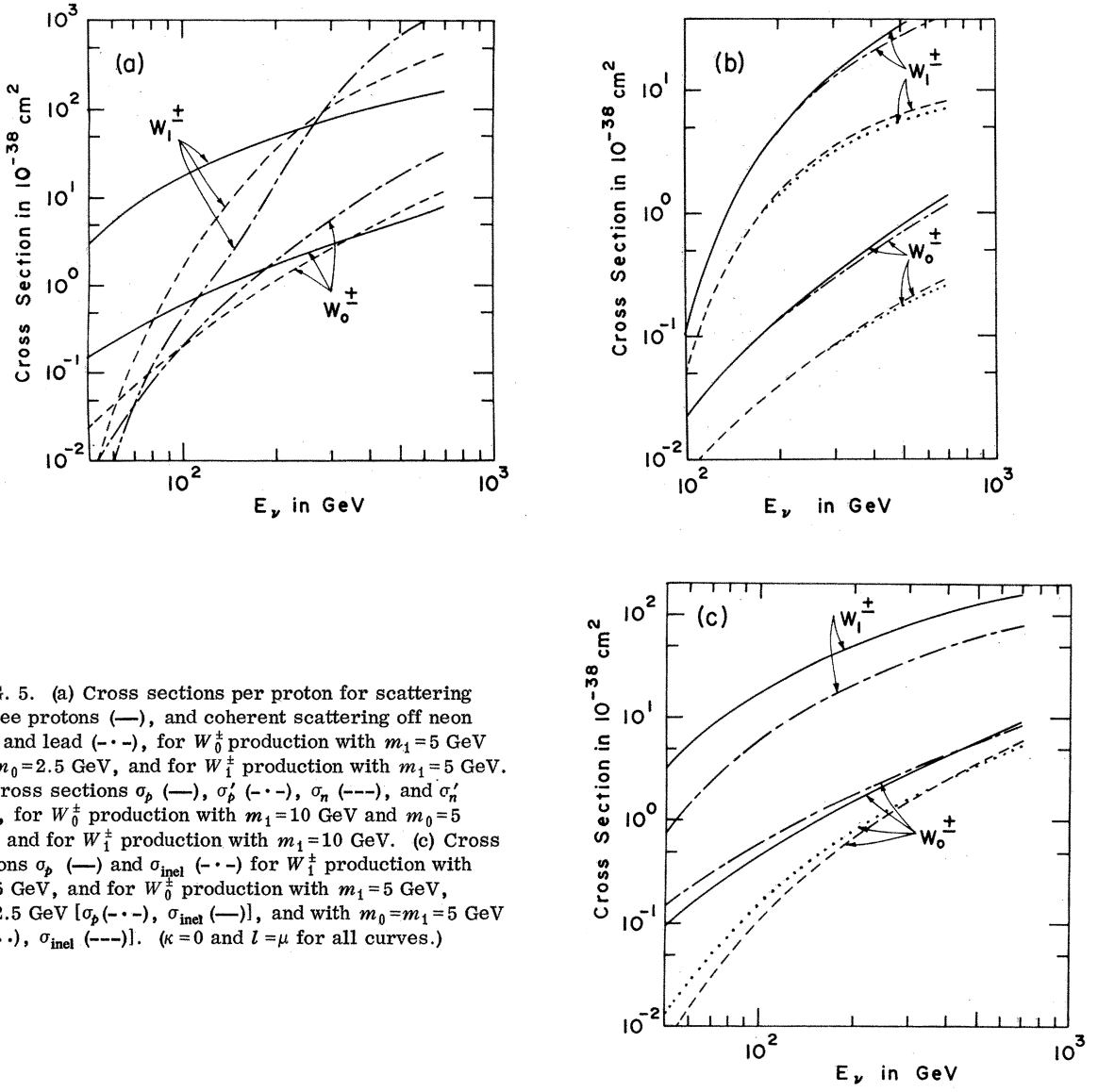

FIG. 5. (a) Cross sections per proton for scattering off free protons (—), and coherent scattering off neon (---) and lead (-·-), for $W_0^\pm$ production with $m_1 = 5$ GeV and $m_0 = 2.5$ GeV, and for $W_1^\pm$ production with $m_1 = 5$ GeV. (b) Cross sections σ_p (—), σ_p' (-·-), σ_n (---), and σ_n' (···), for $W_0^\pm$ production with $m_1 = 10$ GeV and $m_0 = 5$ GeV, and for $W_1^\pm$ production with $m_1 = 10$ GeV. (c) Cross sections σ_p (—) and σ_{inel} (-·-) for $W_1^\pm$ production with $m_1 = 5$ GeV, and for $W_0^\pm$ production with $m_1 = 5$ GeV, $m_0 = 2.5$ GeV [σ_p (-·-), σ_{inel} (—)], and with $m_0 = m_1 = 5$ GeV [σ_p (···), σ_{inel} (---)]. ($\kappa = 0$ and $l = \mu$ for all curves.)

APPENDIX A

The limits of integration for the B^0 calculation are obtained as follows.

The azimuthal angles ϕ_p, and ϕ' are integrated from 0 to 2π. The limits on β (denoted $\beta_\pm$) arise from the constraint

$$|\cos\theta'| \leq 1, \tag{A1}$$

where $\theta' = \angle(\vec{k}, \vec{k}')$ in the frame $\vec{k}' = -\vec{k}_B$. Thus,

$$\beta_\pm = u + (2u + m_l^2 - t)^{-1}\{(m_B^2 - m_l^2)(t-u) \pm (u^2 + m_l^2 t)^{1/2}[(2u - m_B^2 - t)^2 - 4m_l^2 m_B^2]^{1/2}\}. \tag{A2}$$

For the case of elastic scattering off a nucleon, or of coherent scattering off a nucleus, the p'^2 integration is removed by the δ-function constraint $p'^2 = -M^2$. For the case of inelastic scattering off a proton, on the other hand, the minimum allowed value for $|p'^2|$ occurs when Z' consists of a nucleon and pion at rest in their c.m. frame,

$$|p'^2|_- = (M + m_\pi)^2. \tag{A3}$$

The maximum allowed $|p'^2|$ occurs when Z' comes out forward in the lab frame ($\vec{q} \| \vec{k}$):

$$|p'^2|_+ = M^2 - t + (2M/m_l^2) \times [|\vec{k}|_{\text{lab}}(u^2 + m_l^2 t)^{1/2} - u k_{0,\text{lab}}]. \tag{A4}$$

To avoid truncation errors resulting from the near cancellation of large quantities (because m_l is small), the following equivalent expression is used instead of Eq. (A4):

$$|p'^2|_+ = M^2 - t + \frac{2M(|\vec{k}|_{lab}^2 t - u^2)}{|\vec{k}|_{lab}(u^2 + m_l^2 t)^{1/2} + uk_{0,lab}}. \quad \text{(A5)}$$

The lower limit for u is attained when $\beta_- = \beta_+$; thus

$$u_- = \tfrac{1}{2}(t + m_B^2) + m_l m_B. \quad \text{(A6)}$$

The upper limit is reached when $|p'^2|_- = |p'^2|_+$ (in the inelastic case), or when $\vec{q} \| \vec{k}$ (in the elastic or coherent case). This limit is

$$u_+ = |\vec{k}|_{lab}\left[t + \left(\frac{t+\lambda}{2M}\right)^2\right]^{1/2} - k_{0,lab}\left(\frac{t+\lambda}{2M}\right), \quad \text{(A7)}$$

where $\lambda = 0$ for elastic or coherent scattering and $\lambda = 2Mm_\pi + m_\pi^2$ for inelastic scattering off protons.

The variable t is integrated from t_- to t_+, where $t_\pm$ are obtained by setting $u_+ = u_-$; $t_\pm$ are therefore roots of the quadratic equation

$$at^2 + bt + c = 0,$$

with

$$a = \frac{1}{4}\left(\frac{2k_{0,lab}}{M} + 1 + \frac{m_l^2}{M^2}\right),$$

$$b = -k_{0,lab}^2 + \frac{k_{0,lab}}{M}(\eta + \tfrac{1}{2}\lambda) + \eta + m_l^2\left(1 + \frac{\lambda}{2M^2}\right), \quad \text{(A8)}$$

$$c = \frac{k_{0,lab}\eta\lambda}{M} + \eta^2 + \frac{m_l^2\lambda^2}{4M^2},$$

and

$$\eta = \tfrac{1}{2}m_B^2 + m_l m_B. \quad \text{(A9)}$$

The threshold energy for process (1.1) is

$$(k_{0,lab})_- = [\tfrac{1}{2}\lambda + \eta + (m_B + m_l)(M + m')]/M, \quad \text{(A10)}$$

where $m' \equiv 0$ for elastic or coherent scattering, and $m' \equiv m_\pi$ for inelastic scattering off protons.

For $W_J^\pm$ calculations ($J = 0, 1$) the above expressions are changed slightly, since the incoming lepton is no longer of mass m_l. Specifically, Eq. (A2) is replaced by

$$\beta_\pm = u + (2u - t)^{-1}\{(m_J^2 - m_l^2)(t - u) \pm u[(2u - t - m_J^2 - m_l^2)^2 - 4m_l^2 m_J^2]^{1/2}\}; \quad \text{(A11)}$$

Eq. (A4) or (A5) is replaced by

$$|p'^2|_+ = M^2 - t + Mk_{0,lab}t/u - Mu/k_{0,lab}; \quad \text{(A12)}$$

Eq. (A6) by

$$u_- = \tfrac{1}{2}[t + (m_J + m_l)^2]; \quad \text{(A13)}$$

and a, b, and c of Eq. (A8) by

$$a = \frac{k_{0,lab}}{2M} + \frac{1}{4},$$

$$b = -k_{0,lab}^2 + \frac{k_{0,lab}}{M}(\eta' + \tfrac{1}{2}\lambda) + \eta', \quad \text{(A14)}$$

$$c = \frac{k_{0,lab}\eta'\lambda}{M} + \eta'^2,$$

where

$$\eta' = \tfrac{1}{2}(m_J + m_l)^2. \quad \text{(A15)}$$

Equations (A3) and (A7) remain unchanged. The threshold energy is given by Eq. (A10) with the replacements $m_B \to m_J$ and $\eta \to \eta'$.

APPENDIX B

The results of the SCHOONSCHIP trace calculations for the B^0 process are [see Eq. (2.12)]

$$L_{\sigma\sigma} = (-4tm_B^2 + 8m_l^2 m_B^2 - 8m_l^2 t + 16m_l^4)/\beta^2 + (16tm_B^2/y + 8t - 8t^2/y - 8m_B^4/y - 8m_B^2 - 4y - 16m_l^2 + 32m_l^4/y)/\beta + 8t/y - 4tm_B^2/y^2 - 8m_B^2/y - 8tm_l^2/y^2 - 16m_l^2/y + 8m_B^2 m_l^2/y^2 + 16m_l^4/y^2 - 4\beta/y \quad \text{(B1)}$$

and

$$k_\sigma L_{\sigma\tau} k_\tau = [2tm_B^4 - 2m_B^6 - 2ym_B^4 + m_l^2(2tm_B^2 + 4m_B^4) + m_l^4(-4t + 8m_B^2 + 8y) - 16m_l^6]/\beta^2 + [4tm_B^2 - 6m_B^4 - 4ym_B^2 + m_l^2(12t - 4t^2/y + 8m_B^4/y + 4m_B^2 - 6y) + m_l^4(-24t/y + 32) - 32m_l^6/y]/\beta + 2t - 6m_B^2 - 2y + m_l^2(4t/y - 2tm_B^2/y^2 + 12m_B^2/y - 4) + m_l^4(-4t/y^2 + 24/y - 8m_B^2/y^2) - 16m_l^6/y^2 + (-2 + 2m_l^2/y)\beta, \quad \text{(B2)}$$

where

$$y = t - 2u. \quad \text{(B3)}$$

*Research supported in part by the National Aeronautics and Space Administration and the U. S. Atomic Energy Commission.

[1]T. D. Lee, in *Topical Conference on Weak Interactions, CERN, Geneva, 1969* (CERN, Geneva, 1969), p. 427.

[2]T. D. Lee and G. C. Wick, Phys. Rev. D 2, 1033 (1970).

[3]T. D. Lee, Phys. Rev. Letters 25, 1144 (1970). In order to reduce the divergence difficulties in higher-order weak processes, the $W_0^{\pm}$ and $W_1^{\pm}$ are assumed to be of opposite metric.

[4]For kinematic configurations in which $(k-k')^2$ is large, the neglect of these (Compton-type) diagrams is a reasonably good approximation. At first sight, one might have thought that because the lower limit on $(k-k')^2$ is $O(m_l^2)$, where m_l is the lepton mass, contributions from these diagrams at small $(k-k')^2$ could significantly affect the total cross section. However, more detailed calculations (to be published elsewhere) based upon a simple model of the hadronic interactions, suggest that this is not the case for elastic scattering off protons. The contribution of these diagrams to the cross section (for the case $Z=Z'=p$) may typically be two or more orders of magnitude smaller than the contributions of the diagrams of Fig. 1. This occurs because the assumed dipole form factor strongly suppresses emission of the massive B^0 by the proton.

The Compton-type diagrams are not negligible for the case of inelastic scattering off protons. Calculations based on the parton model show that the inelastic cross section (σ'_{inel}) for emission of the B^0 by a proton composed of spin-$\frac{1}{2}$ partons, is comparable to the cross section (σ_{inel}) for emission of the B^0 by the lepton. (The computation of σ_{inel} is described in Sec. III D.) Specifically, $\sigma'_{\text{inel}}/\sigma_{\text{inel}} \cong O(1-2)\langle\sum Q_i^4\rangle/\langle\sum Q_i^2\rangle$, where Q_i are the parton charges.

[5]T. D. Lee, invited talk given at the Amsterdam International Conference on Elementary Particles, 1971 (unpublished); see especially Refs. 11, 16, and 17 of that paper.

[6]R. Linsker, Phys. Rev. Letters 27, 167 (1971).

[7]Throughout the paper, $\hbar=c=1$, $e^2\cong 4\pi/137$, and $g^2=Gm_1^2/\sqrt{2}$, where $G\cong 1.01\times10^{-5}/M_N^2$. The metric used is such that $a\cdot b=\vec{a}\cdot\vec{b}+a_4b_4$, $a_4=ia_0$. All γ matrices are Hermitian.

[8]See, for example, S. Drell and J. D. Walecka, Ann. Phys. (N.Y.) 28, 18 (1964).

[9]M. Veltman (unpublished).

[10]D. H. Coward *et al.*, Phys. Rev. Letters 20, 292 (1968); W. K. H. Panofsky, in *Proceedings of the Fourteenth International Conference on High-Energy Physics, Vienna, 1968,* edited by J. Prentki and J. Steinberger (CERN, Geneva, 1968), p. 23.

[11]J. S. Bell and M. Veltman, Phys. Letters 5, 94 (1963).

[12]J. Løvseth and M. Radomski, Phys. Rev. D 3, 2686 (1971).

[13]R. W. Brown and J. Smith, Phys. Rev. D 3, 207 (1971).

[14]T. D. Lee, P. Markstein, and C. N. Yang, Phys. Rev. Letters 7, 429 (1961).

[15]I. Sick and J. S. McCarthy, Nucl. Phys. A150, 631 (1970), cited in Fig. 3 of Ref. 12.

[16]J. I. Friedman *et al.*, SLAC Report No. SLAC-PUB-907, 1971 (unpublished), Eqs. (2) and (3).

[17]E. D. Bloom and F. J. Gilman, Phys. Rev. Letters 25, 1140 (1970).

[18]The tables used are interpolations of preliminary working data from the SLAC Group A-MIT Collaboration; they were supplied in computer printout form by Richard Early. The experiments are described in the doctoral theses of Guthrie Miller and Martin Breidenbach.

[19]F. Gilman, in *Proceedings of the Fourth International Symposium on Electron and Photon Interactions at High Energies, Liverpool, England, 1969,* edited by D. W. Braben and R. E. Rand (Daresbury Nuclear Physics Laboratory, Daresbury, Lancashire, England, 1970), p. 177.

[20]This approximation ignores effects due to nucleon motion within the target nucleus. These effects have been computed by von Gehlen (Ref. 21) and others for the case of $W_1^{\pm}$ production. Since the c.m. energy of the incident lepton and the nucleon off of which it scatters can be greater when the nucleon has an initial motion than when it is at rest, the threshold energy in the lab frame for quasielastic scattering becomes slightly less than that given by Eq. (A10). The main effect of nucleon motion upon the computed cross section is to increase it very near threshold.

[21]G. von Gehlen, Nuovo Cimento 30, 859 (1963).

[22]E. D. Bloom *et al.*, MIT-SLAC Report No. SLAC-PUB-796, 1970 (unpublished), presented at the Fifteenth International Conference on High Energy Physics, Kiev, U.S.S.R., 1970.

[23]See, for example, Fig. 3 of Ref. 12.

[24]This choice of m_B is suggested by speculations of T. D. Lee, Phys. Rev. Letters 26, 801 (1971).

[25]R. Linsker, Columbia University Report No. NYO-1932(2)-199, 1971 (unpublished); also J. Reiff, Nucl. Phys. B28, 495 (1971); B28, 640(E) (1971). Reiff and the author carried out independent calculations which differed by a factor of $(m_1/m_0)^2$; as a result of communication with Reiff, the error was found in his calculations. The validity of the results presented here has since been confirmed in part by the work of W. Cooper (private communication) and J. Smith (private communication). $W_0^{\pm}$ results have also been reported by M. S. Turner and B. C. Barish, Phys. Rev. D 5, 638 (1972).

[26]See also A. C. T. Wu, C. P. Yang, K. Fuchel, and S. Heller, Phys. Rev. Letters 12, 57 (1964); A. C. T. Wu and C. P. Yang, Phys. Rev. D 1, 3180 (1970); F. Berends and G. B. West, *ibid.* 1, 122 (1970); 2, 1354(E) (1970); 3, 262 (1971); R. W. Brown, A. K. Mann, and J. Smith, Phys. Rev. Letters 25, 257 (1970); J. Reiff, Nucl. Phys. B23, 387 (1970); H. H. Chen, Phys. Rev. D 1, 3197 (1970); Nuovo Cimento 69A, 585 (1970).